

Multiobjective Controller Design by Solving a Multiobjective Matrix Inequality Problem

Wei-Yu Chiu

Abstract

In this study, linear matrix inequality (LMI) approaches and multiobjective (MO) evolutionary algorithms are integrated to design controllers. An MO matrix inequality problem (MOMIP) is first defined. A hybrid MO differential evolution (HMODE) algorithm is then developed to solve the MOMIP. The hybrid algorithm combines deterministic and stochastic searching schemes. In the solving process, the deterministic part aims to exploit the structures of matrix inequalities, and the stochastic part is used to fully explore the decision variable space. Simulation results show that the HMODE algorithm can produce an approximated Pareto front (APF) and Pareto-efficient controllers that stabilize the associated controlled system. In contrast with single-objective designs using LMI approaches, the proposed MO methodology can clearly illustrate how the objectives involved affect each other, i.e., a broad perspective on optimality is provided. This facilitates the selecting process for a representative design, and particularly the design that corresponds to a nondominated vector lying in the knee region of the APF. In addition, controller gains can be readily modified to incorporate the preference or need of a system designer.

W.-Y. Chiu is with the Multiobjective Control Lab, Department of Electrical Engineering, Yuan Ze University, Taoyuan 32003, Taiwan (email: wychiu@saturn.yzu.edu.tw).

This work was supported by the Ministry of Science and Technology of Taiwan under Grant 102-2218-E-155-004-MY3.

This paper is a postprint of a paper submitted to and accepted for publication in IET Control Theory and Applications and is subject to Institution of Engineering and Technology Copyright. The copy of record is available at IET Digital Library.

doi: 10.1049/iet-cta.2014.0026

I. INTRODUCTION

Controller design problems with multiple objectives have been extensively investigated because real-world designs mostly involve multiple objectives that need to be achieved [1]–[3]. In the literature, attaining multiple objectives in a control system has been interpreted differently, yielding various multiobjective (MO) design approaches. For example, in [4] and [5], an MO controller design means that the resulting controller should satisfy some inequality constraints related to several aspects of system performance. In this case, the design procedure does not involve minimising any cost functions (or objective functions) in the objective space. Furthermore, bounds on system specifications are often prescribed rather than being assigned through an optimisation process.

In certain scenarios, an MO design leads to solving a minimisation problem with only one cost function [6]–[12]. A series of single-objective (SO) formulations is mostly used, e.g., linear weighting methods, weighted geometric mean approaches, boundary intersection approaches, and ε -constraint methods [13]–[17]. Although the original design of a control system considers the optimisation of multiple cost functions, an SO problem (SOP) instead of an MO problem (MOP) is solved in the end [18]–[20].

In contrast with the cases in which none or exactly one cost function is involved, an MO design may indeed address two or more cost functions in the design procedure. Existing MO design approaches often employ advanced multiobjective evolutionary algorithms (MOEAs) to evaluate design parameters [21]–[24], yielding an approximated Pareto front (APF). System designers thus have an advantage of being able to understand how multiple objectives affect each other as compared to SO designs. In this scenario, each point or vector on the APF associates with a Pareto-efficient design. The availability of the APF allows the designer to incorporate their preference models into the selecting process for the “optimal” trade-off design. These advantages cannot be achieved through solving a SOP.

Based on above discussions, using an MOEA to solve an MOP for parameter evaluation can be a promising design approach. For controller designs, linear matrix inequality (LMI) approaches have been widely applied to system designs [25], e.g., predictive control designs [26], [27], estimation/observer designs [28], [29], and nonlinear system designs [30]. It becomes constructive to combine these two tools to develop an MO design approach. In [29], an attempt was made to design a networked system (not a control system) with multiple objectives, but a few restrictions on the associated MOP were imposed. For instance, only two objectives can be involved, and the resulting MOP must reduce to an eigenvalue problem after one objective is removed. These restrictions impede the application of the proposed methodology in a general setting. Further research is needed.

In this paper, we aim to integrate MOEAs and LMI approaches for MO controller designs. To this end, a multiobjective matrix inequality problem (MOMIP) is defined. An MOEA termed hybrid multiobjective differential evolution (HMODE) algorithm is then proposed to solve it. Once the MOMIP has been solved, Pareto optimality can be achieved by producing Pareto-efficient controllers. In our framework, the form of the MOMIP results from using LMI approaches in consideration of multiple objectives. It is basically an MOP with matrix inequalities (MIs) as constraints. In such an MOP, two types of decision variables, matrix and non-matrix decision variables, are involved. Regarding the hybrid algorithm, it adopts both stochastic and deterministic searching schemes, i.e., differential evolution (DE) algorithms and interior-point methods, respectively. During the solving process, the former and latter schemes are used to determine the non-matrix and the matrix decision variables, respectively.

The main contributions of this study are as follows. We integrate LMI approaches and MOEAs for controller designs in consideration of multiple objectives, which has not been thoroughly investigated in the literature. The MOMIP is defined and the novel HMODE algorithm is proposed to solve it. By doing so, we connect the evolutionary algorithms field with the control field by providing a framework for the development of hybrid MOEAs that are applicable to MO controller designs.

The following notation is used throughout this paper. The sets of positive integers and real numbers are denoted by \mathbb{Z}_+ and \mathbb{R} , respectively. For a matrix \mathbf{A} , $\mathbf{A} > 0$ means that \mathbf{A} is symmetric and positive-definite. We further define $\mathbf{A} < 0$ as $-\mathbf{A} > 0$. To simplify our notation, the star mark “ \star ” is used in the following two ways:

$$\begin{bmatrix} \mathbf{A} & \star \\ \mathbf{B} & \mathbf{C} \end{bmatrix} = \begin{bmatrix} \mathbf{A} & \mathbf{B}^T \\ \mathbf{B} & \mathbf{C} \end{bmatrix} \text{ and } (\mathbf{A}, \star) = \mathbf{A} + \mathbf{A}^T$$

for appropriate dimensions of matrices \mathbf{A} , \mathbf{B} , and \mathbf{C} . For the terminology of Pareto optimality, i.e., the Pareto dominance, the Pareto optimal set, and the Pareto front, the reader can refer to [17].

The rest of this paper is organized as follows. In Section II, we define the MOMIP and derive its equivalent form. Design examples are presented in Section III. The HMODE algorithm is developed in Section IV. Finally, Section VI concludes this paper.

II. MULTI-OBJECTIVE MATRIX INEQUALITY PROBLEM (MOMIP)

In our MO design approach, the MOMIP is defined as

$$\begin{aligned} & \min_{\alpha, \mathbf{X}} \mathbf{f}(\alpha) \\ & \text{subject to } \mathcal{MI}(\alpha, \mathbf{X}) < 0. \end{aligned} \tag{1}$$

In (1),

$$\boldsymbol{\alpha} = \begin{bmatrix} \alpha_1 & \alpha_2 & \cdots & \alpha_M \end{bmatrix}^T \in \mathbb{R}^M \text{ and } \mathbf{f}(\boldsymbol{\alpha}) \in \mathbb{R}^N \quad (2)$$

represent the vector of all non-matrix decision variables and the vector-valued objective function, respectively. The \mathbf{X} represents a collection of matrix decision variables. The $\mathcal{MI}(\boldsymbol{\alpha}, \mathbf{X})$ denotes a matrix-valued function, and the condition $\mathcal{MI}(\boldsymbol{\alpha}, \mathbf{X}) < 0$ represents MI constraints. Regarding the cost function $\mathbf{f}(\boldsymbol{\alpha})$, it can be a vector of H_∞ attenuation levels when an H_∞ design is adopted. For optimal control, each entry of $\mathbf{f}(\boldsymbol{\alpha})$ can represent an upper bound on a quadratic performance function. For a mixed H_2/H_∞ design, $\mathbf{f}(\boldsymbol{\alpha})$ can represent a mix of performance indices. Regarding the associated MI

$$\mathcal{MI}(\boldsymbol{\alpha}, \mathbf{X}) < 0 \quad (3)$$

the following assumption is made.

Assumption 1: The MI problem (3) is convex in the variable \mathbf{X} once $\boldsymbol{\alpha}$ is given.

In Assumption 1, the convexity in \mathbf{X} originates from the fact that many SO control problems can be designed by solving a convex LMI problem (LMIP). It should be noted that Assumption 1 does not imply that (3) is convex in both \mathbf{X} and $\boldsymbol{\alpha}$. It will become clear that by using LMI approaches, controller design problems with multiple objectives can naturally lead to (1).

For the purpose of algorithm development, we derive another form that is equivalent to the MOMIP (1). The HMODE algorithm will be developed based on the derived form. To begin with the derivation, let us consider conventional SO designs that adopt LMI approaches, yielding the eigenvalue problem (EVP)

$$(\lambda^*(\boldsymbol{\alpha}), \mathbf{X}^*(\boldsymbol{\alpha})) = \begin{array}{l} \arg_{\lambda, \mathbf{X}} \min_{\lambda, \mathbf{X}} \lambda \\ \text{subject to } \mathcal{MI}(\boldsymbol{\alpha}, \mathbf{X}) < \lambda \mathbf{I}. \end{array} \quad (4)$$

In (4), the bound λ on the maximum eigenvalue of the matrix $\mathcal{MI}(\boldsymbol{\alpha}, \mathbf{X})$ is minimised. Here, $\mathbf{X}^*(\boldsymbol{\alpha})$ represents the matrix variable that achieves the minimum $\lambda^*(\boldsymbol{\alpha})$. It is noted that, while $\boldsymbol{\alpha}$ is the non-matrix decision variable in the MOMIP (1), it is not a decision variable in (4). The values of $\lambda^*(\boldsymbol{\alpha})$ and $\mathbf{X}^*(\boldsymbol{\alpha})$ depend on the value of $\boldsymbol{\alpha}$. According to Assumption 1, the EVP (4) is convex in the variable \mathbf{X} given $\boldsymbol{\alpha}$, implying that it can be solved by interior-point methods.

The following lemma relates the feasibility of the MOMIP (1) to the EVP (4).

Lemma 1: If a pair $(\tilde{\boldsymbol{\alpha}}, \tilde{\mathbf{X}})$ is feasible in (1), i.e., $\mathcal{MI}(\tilde{\boldsymbol{\alpha}}, \tilde{\mathbf{X}}) < 0$, then $\mathcal{MI}(\tilde{\boldsymbol{\alpha}}, \mathbf{X}^*(\tilde{\boldsymbol{\alpha}})) < 0$.

Proof: Let λ_{max} be the maximum eigenvalue of $\mathcal{MI}(\tilde{\boldsymbol{\alpha}}, \tilde{\mathbf{X}})$. The condition $\mathcal{MI}(\tilde{\boldsymbol{\alpha}}, \tilde{\mathbf{X}}) < 0$ implies that $\lambda_{max} < 0$ and thus $\mathcal{MI}(\tilde{\boldsymbol{\alpha}}, \tilde{\mathbf{X}}) \leq \lambda_{max} \mathbf{I} < \frac{\lambda_{max}}{2} \mathbf{I} < 0$. The pair $(\frac{\lambda_{max}}{2}, \tilde{\mathbf{X}})$ is a feasible solution of the EVP (4) given $\boldsymbol{\alpha} = \tilde{\boldsymbol{\alpha}}$. By the definitions of $\lambda^*(\cdot)$ and $\mathbf{X}^*(\cdot)$ in (4), we have $\lambda^*(\tilde{\boldsymbol{\alpha}}) \leq \frac{\lambda_{max}}{2} < 0$ and $\mathcal{MI}(\tilde{\boldsymbol{\alpha}}, \mathbf{X}^*(\tilde{\boldsymbol{\alpha}})) < \lambda^*(\tilde{\boldsymbol{\alpha}}) \mathbf{I}$, which completes the proof. ■

With the help of Lemma 1, the following theorem shows that the MOMIP

$$\begin{aligned} & \min_{\alpha} f(\alpha) \\ & \text{subject to } \mathcal{MI}(\alpha, \mathbf{X}^*(\alpha)) < 0 \end{aligned} \quad (5)$$

is equivalent to (1).

Theorem 1: An α^* is a Pareto optimal solution of (5) if and only if there exists a matrix \mathbf{X}' such that (α^*, \mathbf{X}') is a Pareto optimal solution of (1).

Proof: “ \Rightarrow ” Since α^* is Pareto optimal, it is a feasible solution of (5), i.e., $\mathcal{MI}(\alpha^*, \mathbf{X}^*(\alpha^*)) < 0$. By taking $\mathbf{X}' = \mathbf{X}^*(\alpha^*)$, the pair (α^*, \mathbf{X}') is a feasible solution of (1). We now proceed by contraposition. Suppose that there exists a feasible pair (α', \mathbf{X}'') of (1) such that $f(\alpha')$ dominates $f(\alpha^*)$, denoted by $f(\alpha') \prec f(\alpha^*)$. Since $\mathcal{MI}(\alpha', \mathbf{X}'') < 0$, according to Lemma 1, we have $\mathcal{MI}(\alpha', \mathbf{X}^*(\alpha')) < 0$. The conditions $f(\alpha') \prec f(\alpha^*)$ and $\mathcal{MI}(\alpha', \mathbf{X}^*(\alpha')) < 0$ contradict the Pareto optimality of α^* in (5). Therefore, such a pair (α', \mathbf{X}'') does not exist, and the pair (α^*, \mathbf{X}') must be Pareto optimal in (1).

“ \Leftarrow ” Since (α^*, \mathbf{X}') is Pareto optimal, it is feasible in (1) and, according to Lemma 1, α^* is a feasible solution of (5). We proceed by contraposition. Suppose that α^* is not Pareto optimal in (5). There exists a feasible α' , i.e., $\mathcal{MI}(\alpha', \mathbf{X}^*(\alpha')) < 0$, such that $f(\alpha')$ dominates $f(\alpha^*)$, denoted by $f(\alpha') \prec f(\alpha^*)$. Let $\mathbf{X}'' = \mathbf{X}^*(\alpha')$. We have $\mathcal{MI}(\alpha', \mathbf{X}'') < 0$ and $f(\alpha') \prec f(\alpha^*)$, which contradicts the fact that the pair (α^*, \mathbf{X}') is Pareto optimal in (1). Therefore, the feasible α' that dominates α^* in (5) does not exist. We conclude that α^* is Pareto optimal in (5). ■

Theorem 1 is key to the successful application of MOEAs to solving MOMIPs. As the MOMIP (5) is equivalent to (1) according to Theorem 1, we can solve (5) to obtain the design parameters. It is worth noting that \mathbf{X} and α are the decision variables in (1) while α is the only decision variable in (5). To some extent, the MOMIP (5) can be regarded as a conventional MOP with α as the decision variable.

III. DESIGN EXAMPLES

In this section, design examples associated with the MOMIP (5) are investigated.

A. Example 1: Robust Control Design

Consider a robust H_∞ fuzzy control design for the uncertain fuzzy system [31]–[35]

$$\begin{aligned} \dot{\mathbf{x}}(t) &= \sum_{i=1}^{\mathcal{N}_r} \xi_i(\boldsymbol{\nu}(t)) \{ [\mathbf{A}_i + \Delta \mathbf{A}_i] \mathbf{x}(t) + \mathbf{B}_{1_i} \mathbf{w}(t) + \mathbf{B}_{2_i} \mathbf{u}(t) \}, \mathbf{x}(0) = 0 \\ \mathbf{y}(t) &= \sum_{i=1}^{\mathcal{N}_r} \xi_i(\boldsymbol{\nu}(t)) \mathbf{C}_i \mathbf{x}(t) + \mathbf{D}_i \mathbf{u}(t) \end{aligned} \quad (6)$$

where

$$\Delta \mathbf{A}_i = F(\mathbf{x}(t), t) \mathbf{H}_i. \quad (7)$$

In (6), $\mathbf{x}(t)$ represents the state vector, $\mathbf{w}(t)$ the external disturbances, and $\mathbf{y}(t)$ the system output. The fuzzy controller

$$\mathbf{u}(t) = \sum_{i=1}^{\mathcal{N}_r} \xi_i(\boldsymbol{\nu}(t)) \mathbf{K}_i \mathbf{x}(t) \quad (8)$$

is considered, where $\xi_i, i = 1, 2, \dots, \mathcal{N}_r$, represent normalized fuzzy bases, $\boldsymbol{\nu}(t)$ is the premise vector, \mathcal{N}_r is the number of fuzzy rules, and $\mathbf{K}_i, i = 1, 2, \dots, \mathcal{N}_r$, are the controller gains that need to be designed. In (7), $\mathbf{H}_i, i = 1, 2, \dots, \mathcal{N}_r$, are known matrices that characterize the structure of $\Delta \mathbf{A}_i$, and $F(\mathbf{x}(t), t)$ models the uncertainty with

$$\|F(\mathbf{x}(t), t)\| \leq \frac{1}{\rho}. \quad (9)$$

The following lemma shows the LMI formulation for the controller design [35].

Lemma 2: The system (6) has an \mathcal{L}_2 -gain less than or equal to γ , i.e.,

$$\int_0^\infty \mathbf{y}(t)^T \mathbf{y}(t) dt \leq \gamma^2 \int_0^\infty \mathbf{w}(t)^T \mathbf{w}(t) dt, \mathbf{x}(0) = 0 \quad (10)$$

for all

$$\int_0^\infty \mathbf{w}(t)^T \mathbf{w}(t) dt < \infty$$

if there exist a matrix \mathbf{Z} , a positive scalar δ , and matrices $\mathbf{M}_i, i = 1, 2, \dots, \mathcal{N}_r$, such that

$$\mathbf{Z} > 0 \text{ and } \boldsymbol{\Omega}_{ij} + \boldsymbol{\Omega}_{ji} < 0, 1 \leq i \leq j \leq \mathcal{N}_r \quad (11)$$

where

$$\boldsymbol{\Omega}_{ij} = \begin{bmatrix} (\mathbf{A}_i \mathbf{Z}, \star) + (\mathbf{B}_{2_i} \mathbf{M}_j, \star) & \star & \star \\ \tilde{\mathbf{B}}_{1_i}^T & -\gamma \mathbf{I} & \star \\ \tilde{\mathbf{C}}_i \mathbf{Z} + \tilde{\mathbf{D}}_i \mathbf{M}_j & 0 & -\gamma \mathbf{I} \end{bmatrix}$$

with

$$\tilde{\mathbf{B}}_{1_i} = \begin{bmatrix} \delta \mathbf{I} & \mathbf{B}_{1_i} \end{bmatrix}, \tilde{\mathbf{C}}_i = \begin{bmatrix} \frac{\gamma}{\rho \delta} \mathbf{H}_i^T & \sqrt{2} \mathbf{C}_i^T \end{bmatrix}^T, \text{ and } \tilde{\mathbf{D}}_i = \begin{bmatrix} 0 & \sqrt{2} \mathbf{D}_i^T \end{bmatrix}^T. \quad (12)$$

The controller gains $\mathbf{K}_i, i = 1, 2, \dots, \mathcal{N}_r$, can be recovered by $\mathbf{K}_i = \mathbf{M}_i \mathbf{Z}^{-1}$.

Proof: Referring to the proof of Theorem 3.1 in [35], the result follows from using the augmented disturbance

$$\tilde{\mathbf{w}}(t) = \begin{bmatrix} (\frac{1}{\delta} F(\mathbf{x}(t), t) \mathbf{H}_i \mathbf{x}(t))^T & \mathbf{w}(t)^T \end{bmatrix}^T.$$

■

In [35], the values of γ , ρ , and δ have been heuristically prescribed, and a feasibility problem consisting of the constraints (11) has been dealt with. For an SO design, we can minimise the attenuation level γ , and assign the values of the uncertainty tolerance $1/\rho$ in (9) and the auxiliary variable δ in (12) in advance, yielding an LMIP. These conventional design approaches lead to solving a feasibility problem or an SOP.

Suppose that we are interested in the controller gains so that the resulting system can tolerate as much uncertainty as possible and achieve a minimal attenuation level simultaneously. In this scenario, it is desired to maximise $1/\rho$ and minimise γ . Referring to (5), this can be achieved by choosing

$$\boldsymbol{\alpha} = \begin{bmatrix} \gamma & \rho & \delta \end{bmatrix}^T, \mathbf{X}^*(\boldsymbol{\alpha}) = (\mathbf{Z}^*(\boldsymbol{\alpha}), \mathbf{M}_1^*(\boldsymbol{\alpha}), \dots, \mathbf{M}_{\mathcal{N}_r}^*(\boldsymbol{\alpha})), \text{ and } \mathbf{f}(\boldsymbol{\alpha}) = \begin{bmatrix} \gamma & \rho \end{bmatrix}^T. \quad (13)$$

Based on Theorem 1 and Lemma 2, the controller gains

$$\mathbf{K}_i^*(\boldsymbol{\alpha}) = \mathbf{M}_i^*(\boldsymbol{\alpha}) \times [\mathbf{Z}^*(\boldsymbol{\alpha})]^{-1}, i = 1, 2, \dots, \mathcal{N}_r,$$

can be determined by solving

$$\begin{aligned} & \min_{\gamma, \rho, \delta} \begin{bmatrix} \gamma & \rho \end{bmatrix}^T \\ & \text{subject to } \mathbf{Z}^*(\boldsymbol{\alpha}) > 0, \boldsymbol{\Omega}_{ij}^*(\boldsymbol{\alpha}) + \boldsymbol{\Omega}_{ji}^*(\boldsymbol{\alpha}) < 0, \\ & 1 \leq i \leq j \leq \mathcal{N}_r. \end{aligned} \quad (14)$$

Once the MOMIP (14) has been solved, we are able to jointly consider the tolerance of system uncertainty and the H_∞ attenuation level. Furthermore, all the values of γ , ρ , and δ are determined through optimisation rather than a heuristic assignment. These differentiate our MO design approach from conventional ones.

Another advantage of using the proposed methodology is its flexibility to adjust controller gains. Typically, when an H_∞ design is adopted, ‘‘large values’’ of controller gains $\mathbf{K}_i, i = 1, 2, \dots, \mathcal{N}_r$, can result from using a very small value of the H_∞ attenuation level γ . However, too large values of \mathbf{K}_i can be impractical in the implementation. A trial-and-error method that assigns the attenuation level is used mostly to avoid this difficulty. In our MO design approach, we can modify the objective function to reduce the values of controller gains. In this example, it is noted that

$$\mathbf{K}_i^*(\boldsymbol{\alpha}) = \mathbf{M}_i^*(\boldsymbol{\alpha})[\mathbf{Z}^*(\boldsymbol{\alpha})]^{-1} = \mathbf{M}_i^*(\boldsymbol{\alpha}) \times \frac{\text{adj}(\mathbf{Z}^*(\boldsymbol{\alpha}))}{\det(\mathbf{Z}^*(\boldsymbol{\alpha}))}$$

where $\text{adj}(\cdot)$ and $\det(\cdot)$ denote the classical adjoint and the determinant of a square matrix, respectively. Roughly speaking, we may reduce the value of $1/\det(\mathbf{Z}^*(\boldsymbol{\alpha}))$ to avoid obtaining large $\mathbf{K}_i^*(\boldsymbol{\alpha})$. Therefore,

the 3rd objective $1/\det(\mathbf{Z}^*(\boldsymbol{\alpha}))$ is added to the original objective function, yielding the MOMIP

$$\begin{aligned} \min_{\gamma, \rho, \delta} \left[\gamma \quad \rho \quad \frac{1}{\det(\mathbf{Z}^*(\boldsymbol{\alpha}))} \right]^T \\ \text{subject to } \mathbf{Z}^*(\boldsymbol{\alpha}) > 0, \boldsymbol{\Omega}_{ij}^*(\boldsymbol{\alpha}) + \boldsymbol{\Omega}_{ji}^*(\boldsymbol{\alpha}) < 0, \\ 1 \leq i \leq j \leq \mathcal{N}_r. \end{aligned} \quad (15)$$

Our simulations will demonstrate the effectiveness of this method.

B. Example 2: Bounded-Input Bounded-Output (BIBO) System Design

In real-world control problems, bounded outputs and inputs are usually desired. Generally speaking, lowering the upper bound on the input and lowering that on the output are two conflicting objectives. By lowering the upper bound on the control input, less input energy is used. As a result, the output performance can deteriorate, increasing the upper bound on the output.

Consider a linear system

$$\begin{aligned} \dot{\mathbf{x}}(t) &= \mathbf{A}\mathbf{x}(t) + \mathbf{B}\mathbf{u}(t) \\ \mathbf{y}(t) &= \mathbf{C}\mathbf{x}(t). \end{aligned} \quad (16)$$

The following lemma provides LMI conditions for the bounds on the input $\mathbf{u}(t) = \mathbf{K}\mathbf{x}(t)$ and output $\mathbf{y}(t)$ of the control system (16).

Lemma 3: If there exist matrices \mathbf{Z} and \mathbf{M} such that

$$(\mathbf{AZ}, \star) + (\mathbf{BM}, \star) < 0, \mathbf{Z}_1 = \begin{bmatrix} 1 & \star \\ \mathbf{x}(0) & \mathbf{Z} \end{bmatrix} > 0, \mathbf{Z}_2 = \begin{bmatrix} \mathbf{Z} & \star \\ \mathbf{M} & \bar{u}^2 \mathbf{I} \end{bmatrix} > 0, \text{ and } \mathbf{Z}_3 = \begin{bmatrix} \mathbf{Z} & \star \\ \mathbf{CZ} & \bar{y}^2 \mathbf{I} \end{bmatrix} > 0 \quad (17)$$

then the system (16) is quadratically stabilizable with

$$\|\mathbf{u}(t)\| = \|\mathbf{K}\mathbf{x}(t)\| < \bar{u} \text{ and } \|\mathbf{y}(t)\| < \bar{y}$$

using the controller gain $\mathbf{K} = \mathbf{M}\mathbf{Z}^{-1}$.

Proof: The reader can refer to Theorems 11 and 12 in [30] or (7.16) in [25] for a detailed proof. ■

Referring to (5), we let

$$\mathbf{f}(\boldsymbol{\alpha}) = \boldsymbol{\alpha} = \begin{bmatrix} \bar{u} & \bar{y} \end{bmatrix}^T \text{ and } \mathbf{X}^*(\boldsymbol{\alpha}) = (\mathbf{Z}^*(\boldsymbol{\alpha}), \mathbf{M}^*(\boldsymbol{\alpha})).$$

Based on Theorem 1 and Lemma 3, the MOMIP associated with the BIBO system design can be formulated as

$$\begin{aligned} & \min_{\alpha} \alpha \\ & \text{subject to } \mathbf{Z}_1^*(\alpha) > 0, \mathbf{Z}_2^*(\alpha) > 0, \mathbf{Z}_3^*(\alpha) > 0, \\ & (\mathbf{AZ}^*(\alpha), \star) + (\mathbf{BM}^*(\alpha), \star) < 0 \end{aligned} \quad (18)$$

Conventionally, both bounds were assigned in advance, or one bound was minimised with the other bound prescribed. In contrast, our MO approach minimises the upper bounds simultaneously, as shown in (18). This provides the designer with a broader perspective on optimality, and on Pareto optimality in particular.

Due to space limitation, only two design examples have been examined. The proposed methodology can be extended to other optimisation problems with LMI constraints. More examples with possible MO formulations in the form of (1) are discussed as follows. In [36] and [37], the problem of computing the region of attraction (ROA) was investigated. Suppose that the estimation of the ROA of a system has been formulated as an SOP with LMI constraints and that a robust control law is desired to stabilize the system. To apply the proposed MO approach to this scenario, we may maximise the estimated ROA and minimise an H_∞ attenuation level. In [38], the design of dynamic anti-windup compensators was addressed, and design problems having the same LMI constraints but different objectives were formulated as separate LMIPs. Among them, one design aimed at the maximisation of the disturbance tolerance, and another design focused on the maximisation of the disturbance attenuation. For an MO extension, we may consider an MOP in which the disturbance tolerance and the disturbance attenuation are maximised.

In [39] and [40], strictly positive real (SPR) controllers and control systems with ellipsoidal parametric uncertainty were considered, respectively. LMI approaches were employed for controller synthesis in both studies. An H_2 design that addresses the average system performance was adopted in [39], and an H_∞ design that focuses on the robustness of a system in worst-case scenarios was used in [40]. For a mixed H_2/H_∞ design and its MO extension, both H_2 and H_∞ performance indices can be minimised simultaneously in our MO approach. Finally, in [41], model predictive control (MPC) of nonlinear systems was considered. For an MO formulation associated with the MPC problem, minimising the upper bound on the infinite horizon cost and the upper bound on the input energy can be the two objectives. In this case, further research is needed to address the computational complexity for an online application.

IV. PROPOSED HMODE ALGORITHM

As mentioned previously, there are several advantages of solving the MOMIP (1) or its equivalent form (5) for an MO controller design. In this section, we develop an algorithm that can solve (5). Since DE algorithms have been found to be very robust and applied to a large number of SOPs, their basic structure is used in the proposed algorithm. To manage the MI constraints, we integrate interior-point methods into our solution searching scheme, resulting in the hybrid algorithm. Roughly speaking, infeasible solutions ($\lambda^*(\boldsymbol{\alpha}) > 0$, as shown in the proof of Lemma 1) or dominated solutions tend to be removed during the algorithm iteration. Feasible and nondominated solutions are thus remained so that an APF can be obtained when the algorithm stops.

To facilitate the ensuing discussion, let $rand_{(a,b)}$ and $unidrnd_M$ denote continuous and discrete uniform random variables over (a, b) and $\{1, 2, \dots, M\}$, respectively. For column vectors \mathbf{a} and $\mathbf{b} \in \mathbb{R}^N$, the expression $\mathbf{a} < \mathbf{b}$ ($\mathbf{a} \leq \mathbf{b}$) stands for $[\mathbf{a}]_i < [\mathbf{b}]_i$ ($[\mathbf{a}]_i \leq [\mathbf{b}]_i$) for $i = 1, 2, \dots, N$, where $[\cdot]_i$ denotes the i th entry of a vector. Furthermore, $\mathbf{a} \in [\underline{\mathbf{a}}, \bar{\mathbf{a}}]$ implies that $\underline{\mathbf{a}} \leq \mathbf{a}$ and $\mathbf{a} \leq \bar{\mathbf{a}}$. For a matrix \mathbf{A} , $[\mathbf{A}]_{ij}$ denotes its (i, j) th entry. We are now in the position to present the proposed algorithm as follows.

HMODE Algorithm

Input:

- MOMIP (5).
- \mathcal{N}_p , the population size;
- $\mathcal{N}_{\mathcal{I}}$, the number of iterations;
- $\eta_c \in (0, 1)$, control parameter of the crossover;
- η_d , control parameter of the crowding distance;
- $[\underline{\boldsymbol{\alpha}}, \bar{\boldsymbol{\alpha}}]$, the range of interest for the non-matrix decision variable $\boldsymbol{\alpha}$.

Step 1) Initialization:

Step 1.1) Let $\Gamma_f = \emptyset$, the set consisting of the best-so-far vectors in the objective function space; $\Gamma = \emptyset$, the set consisting of matrix and non-matrix variables in the decision variable space (each point in Γ corresponds to a vector stored in Γ_f); and the algorithm counter $t_c = 1$.

Step 1.2) Randomly generate an initial population

$$\boldsymbol{\alpha}_1, \boldsymbol{\alpha}_2, \dots, \boldsymbol{\alpha}_{\mathcal{N}_p} \in [\underline{\boldsymbol{\alpha}}, \bar{\boldsymbol{\alpha}}].$$

Step 2) Differential Evolution:

For $i = 1$ to \mathcal{N}_p **do**

If the Phase-I stage is active, e.g., $t_c \leq \frac{2}{3}\mathcal{N}_{\mathcal{I}}$, **then**

Step 2.I.1) Mutation operation:

$$\mathbf{v}_i = \boldsymbol{\alpha}_{best} + rand_{(0,1)}(i)(\boldsymbol{\alpha}_j - \boldsymbol{\alpha}_k) \quad (19)$$

where j and k are distinct integers and randomly selected from $\mathbb{Z}_+ \cap [1, \mathcal{N}_p] \setminus \{i\}$, and $\boldsymbol{\alpha}_{best}$ is randomly chosen from Γ if $\Gamma \neq \emptyset$. If $\Gamma = \emptyset$, then $\boldsymbol{\alpha}_{best} = \boldsymbol{\alpha}_\ell$ for some integer ℓ randomly selected from $\mathbb{Z}_+ \cap [1, \mathcal{N}_p] \setminus \{i, j, k\}$.

Step 2.I.2) Reflection operation:

$$[\mathbf{v}'_i]_j = \begin{cases} \min\{[\bar{\boldsymbol{\alpha}}]_j, 2[\underline{\boldsymbol{\alpha}}]_j - [\mathbf{v}_i]_j\}, & \text{if } [\mathbf{v}_i]_j < [\underline{\boldsymbol{\alpha}}]_j \\ \max\{[\underline{\boldsymbol{\alpha}}]_j, 2[\bar{\boldsymbol{\alpha}}]_j - [\mathbf{v}_i]_j\}, & \text{if } [\mathbf{v}_i]_j > [\bar{\boldsymbol{\alpha}}]_j \\ [\mathbf{v}_i]_j, & \text{otherwise.} \end{cases} \quad (20)$$

Step 2.I.3) Crossover operation:

$$[\boldsymbol{\varphi}_i]_j = \begin{cases} [\mathbf{v}'_i]_j, & \text{if } rand_{(0,1)}(i, j) \leq \eta_c \text{ or} \\ & j = unidrnd_M(i, j) \\ [\boldsymbol{\alpha}_i]_j, & \text{otherwise.} \end{cases} \quad (21)$$

Step 2.I.4) Selection operation:

Assign

$$\boldsymbol{\alpha}_i = \boldsymbol{\varphi}_i$$

if either

$$\lambda^*(\boldsymbol{\varphi}_i) < 0 < \lambda^*(\boldsymbol{\alpha}_i) \quad (22)$$

or

$$\lambda^*(\boldsymbol{\varphi}_i), \lambda^*(\boldsymbol{\alpha}_i) < 0 \text{ and } \mathbf{f}(\boldsymbol{\varphi}_i) < \mathbf{f}(\boldsymbol{\alpha}_i) \quad (23)$$

holds true.

Else (Phase-II stage is active, e.g., $t_c > \frac{2}{3}\mathcal{N}_T$)

Assign

$$\boldsymbol{\alpha}_i = \mathbf{R}_i \boldsymbol{\alpha}'_i + (\mathbf{I}_M - \mathbf{R}_i) \boldsymbol{\alpha}''_i \quad (24)$$

where \mathbf{I}_M represents the $M \times M$ identity matrix, $\boldsymbol{\alpha}'_i$ and $\boldsymbol{\alpha}''_i$ are distinct vectors randomly selected from Γ , and $\mathbf{R}_i \in \mathbb{R}^{M \times M}$ is defined as

$$[\mathbf{R}_i]_{jk} = \begin{cases} rand_{(0,1)}(i, j), & \text{if } 1 \leq j = k \leq M \\ 0, & \text{otherwise.} \end{cases} \quad (25)$$

End If

End For

Step 3) Update: Let

$$\vartheta(1), \vartheta(2), \dots, \vartheta(\kappa)$$

be the indices of all non-matrix decision variables that are feasible, i.e.,

$$\lambda^*(\alpha_{\vartheta(i)}) < 0, i = 1, 2, \dots, \kappa. \quad (26)$$

For $i = 1$ to κ **do**

If $\mathbf{f}(\alpha_{\vartheta(i)})$ is not dominated by any vectors in Γ_f , **then**

Step 3.1) Remove all

$$\mathbf{f}(\alpha) \in \Gamma_f \text{ and } (\alpha, \mathbf{X}^*(\alpha)) \in \Gamma$$

if $\mathbf{f}(\alpha_{\vartheta(i)})$ dominates $\mathbf{f}(\alpha)$.

Step 3.2) Add $\mathbf{f}(\alpha_{\vartheta(i)})$ to Γ_f and the associated design parameters $(\alpha_{\vartheta(i)}, \mathbf{X}^*(\alpha_{\vartheta(i)}))$ to Γ if

$$\|\mathbf{f}(\alpha_{\vartheta(i)}) - \Gamma_f\| > \eta_d \quad (27)$$

where $\|\mathbf{f}(\alpha_{\vartheta(i)}) - \Gamma_f\|$ represents the Euclidean distance between the vector $\mathbf{f}(\alpha_{\vartheta(i)})$ and the set Γ_f .

End If

End For

Step 4) Stopping Criterion: Set $t_c = t_c + 1$. If $t_c \leq \mathcal{N}_{\mathcal{I}}$, then go to **Step 2)**. Otherwise, go to **Step 5)**.

Step 5) Knee Selection: Evaluate

$$\alpha^* = \arg_{\alpha} \max_{\mathbf{f}(\alpha) \in \Gamma_f} \prod_{n=1}^N \frac{\bar{f}_n - [\mathbf{f}(\alpha)]_n}{\bar{f}_n - \underline{f}_n} \quad (28)$$

where

$$\bar{f}_n = \max_{\mathbf{f}(\alpha) \in \Gamma_f} [\mathbf{f}(\alpha)]_n \text{ and } \underline{f}_n = \min_{\mathbf{f}(\alpha) \in \Gamma_f} [\mathbf{f}(\alpha)]_n$$

for $n = 1, 2, \dots, N$.

Output:

- Γ_f , the APF.
- $\mathbf{f}(\alpha^*)$, the knee selected from Γ_f .
- $(\alpha^*, \mathbf{X}^*(\alpha^*))$, the design parameters selected from Γ .

Several points regarding the proposed algorithm are addressed in the following paragraphs.

For the inputs of the proposed HMODE algorithm, we often have $\underline{\alpha} > 0$ for the range of interest $[\underline{\alpha}, \bar{\alpha}]$ as each entry of the vector α mostly represents a certain performance index. In Step 1.1), the sets Γ_f and Γ have been used to store best-so-far vectors and the corresponding design parameters, respectively. The structures of these sets are clear from Step 3.1), i.e.,

$$\Gamma_f \subset \{\mathbf{f}(\alpha) : \alpha \in [\underline{\alpha}, \bar{\alpha}]\} \text{ and } \Gamma = \{(\alpha, \mathbf{X}^*(\alpha)) : \mathbf{f}(\alpha) \in \Gamma_f\}.$$

It is well-known that DE algorithms have a fast convergence rate but they often reach the vicinity of the true Pareto front [17], [42]. To overcome this problem and maintain the convergence rate, a two-phase scheme has been proposed in [43]. Motivated by the idea of using a two-phase scheme, we have adopted the basic structure of conventional DE algorithms at our Phase-I stage, and performed a crossover operation (24) over best-so-far solutions at the Phase-II stage. The Phase-I and Phase-II stages are used to address the exploration and exploitation of a search space, respectively. These stages are key to finding feasible and nondominated solutions.

In Step 2.I.1), there are several ways to calculate the mutant, e.g., “DE/rand/1”, “DE/best/1”, “DE/current-to-best/1”, and “DE/current-to-rand/1” [44], [45]. In general, α_{best} in (19) should yield good performance in the objective function space to achieve fast convergence in the mutating process. For an SOP, “good performance” means that α_{best} can achieve a small objective value. In the proposed algorithm, solutions in Γ corresponding to best-so-far vectors in Γ_f serve as α_{best} .

To ensure that mutants satisfy the range of interest $[\underline{\alpha}, \bar{\alpha}]$, the modification (20) in Step 2.I.2) has been performed [46]. This is termed the reflection operation because $[v_i]_j$ is reflected to $[v'_i]_j$ about $[\underline{\alpha}]_j$ if $[v_i]_j < [\underline{\alpha}]_j$ and about $[\bar{\alpha}]_j$ if $[v_i]_j > [\bar{\alpha}]_j$. It is evident from (19) and (20) that the mutant v'_i satisfies $v'_i \in [\underline{\alpha}, \bar{\alpha}]$. Similarly, the offspring φ_i produced from the crossover operation (21) in Step 2.I.3) satisfies $\varphi_i \in [\underline{\alpha}, \bar{\alpha}]$. In Step 2.I.4), the offspring φ_i is selected if it is better than its predecessor, i.e., either (22) or (23) holds true, each of which requires that φ_i be feasible, i.e., $\lambda^*(\varphi_i) < 0$. By using the selection operation defined in Step 2.I.4), conventional DE algorithms for SO optimisation have been extended to address the MOMIP.

At the Phase-II stage, we explore the neighborhood of solutions in Γ using (24) in order to reach the true Pareto front. Due to the design of $[\mathbf{R}_i]_{jk}$ in (25), the newly produced offspring α_i in (24) can be regarded as a point randomly chosen from the cube

$$\prod_{j=1}^M [\min\{[\alpha'_i]_j, [\alpha''_i]_j\}, \max\{[\alpha'_i]_j, [\alpha''_i]_j\}]. \quad (29)$$

Fig. 1 shows the graphical illustration of the cube defined in (29) for $M = 3$. Analogous to the property

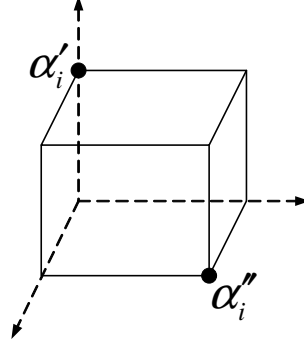


Fig. 1. Illustration of the cube in (29) for $M = 3$. In this case, the offspring α_i of α'_i and α''_i produced by (24) is a point within this cube.

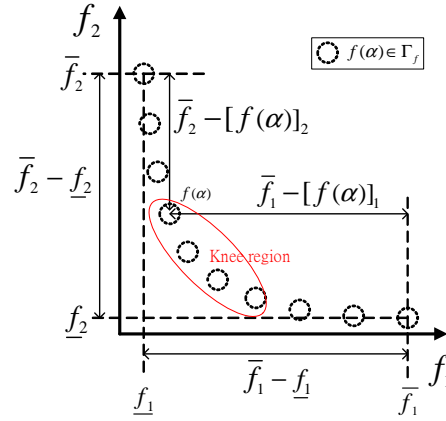


Fig. 2. Diagram of (28) with $N = 2$. For the n th objective, the value $\bar{f}_n - [f(\alpha)]_n$ represents the improvement achieved by the solution α , and the value $\bar{f}_n - \underline{f}_n$ represents the maximum improvement with respect to Γ_f .

that v'_i and φ_i are always confined within $[\underline{\alpha}, \bar{\alpha}]$, we have $\alpha_i \in [\underline{\alpha}, \bar{\alpha}]$ for all i at the Phase-II stage. We conclude that

$$v'_i = v'_i(t_c) \in [\underline{\alpha}, \bar{\alpha}], \varphi_i = \varphi_i(t_c) \in [\underline{\alpha}, \bar{\alpha}], \text{ and } \alpha_i = \alpha_i(t_c) \in [\underline{\alpha}, \bar{\alpha}]$$

for all i and t_c .

In Step 3), the update process is active only if feasible solutions have been found, i.e., the conditions (26) hold true for a positive integer κ . To maintain a manageable size of the APF, a simple mechanism (27) has been introduced: if $f(\alpha)$ is not dominated by any vectors in Γ_f and poses a distance away from the set Γ_f , then $f(\alpha)$ and $(\alpha, X^*(\alpha))$ enter the external archives Γ_f and Γ , respectively. In Step 4), once t_c , the counter of the number of iterations, has exceeded the prescribed $\mathcal{N}_{\mathcal{I}}$, the DE in Step 2) will no

longer be executed, and a set of design parameters becomes available. The aim of the remaining work is to choose the most reasonable design for the control system.

In Step 5), the final design has been selected by the optimisation process (28) that fully exploits the knowledge extracted from the APF Γ_f . Since knee solutions are often preferred, the chosen design should be able to reflect this preference. To illustrate the underlying idea of using (28), Fig. 2 presents a case in which two objectives are involved. In such a case, the quantities

$$\frac{\bar{f}_1 - [\mathbf{f}(\boldsymbol{\alpha})]_1}{\bar{f}_1 - \underline{f}_1} \text{ and } \frac{\bar{f}_2 - [\mathbf{f}(\boldsymbol{\alpha})]_2}{\bar{f}_2 - \underline{f}_2} \quad (30)$$

can be interpreted as the normalized improvement with respect to the first and second objectives, respectively. According to (28), the design that maximises the ‘‘overall improvement’’ will be selected, in which the overall improvement is defined as the the product of the separate improvement of each objective, i.e., the product of the two terms in (30). To some extent, the optimisation process (28) aims to create a win-win situation by searching for the ‘‘optimal’’ design that sacrifices each objective to some degree in order to do well on the whole.

In the end of the proposed HMODE algorithm, we output valuable information Γ_f and $\mathbf{f}(\boldsymbol{\alpha}^*)$, allowing the designer of control systems to have a good understanding of the chosen design parameters $(\boldsymbol{\alpha}^*, \mathbf{X}^*(\boldsymbol{\alpha}^*))$.

V. NUMERICAL EXAMPLES

This section provides a simulation study of the proposed methodology. The values $\mathcal{N}_p = 100, \mathcal{N}_{\mathcal{I}} = 200, \eta_c = 0.2$, and $\eta_d = 0.05$ have been chosen as the inputs to the HMODE algorithm. The proposed algorithm has been applied to solving the MOMIPs in the design examples in Section III.

A. Example 1: Robust Control Design

Consider the chaotic Lorenz system [34], [35]

$$\begin{aligned} \dot{x}_1(t) &= -\sigma x_1(t) + \sigma x_2(t) + u(t) + 0.1w_1(t) \\ \dot{x}_2(t) &= rx_1(t) - x_2(t) - x_1(t)x_3(t) + 0.1w_2(t) \\ \dot{x}_3(t) &= x_1(t)x_2(t) - bx_3(t) + 0.1w_3(t) \\ \mathbf{y}(t) &= \left[x_1(t) + u(t) \quad x_2(t) + u(t) \quad x_3(t) + u(t) \right]^T \end{aligned} \quad (31)$$

where σ, r , and b are uncertain parameters with the nominal values

$$\sigma \approx 10, r \approx 28, \text{ and } b \approx 8/3 \quad (32)$$

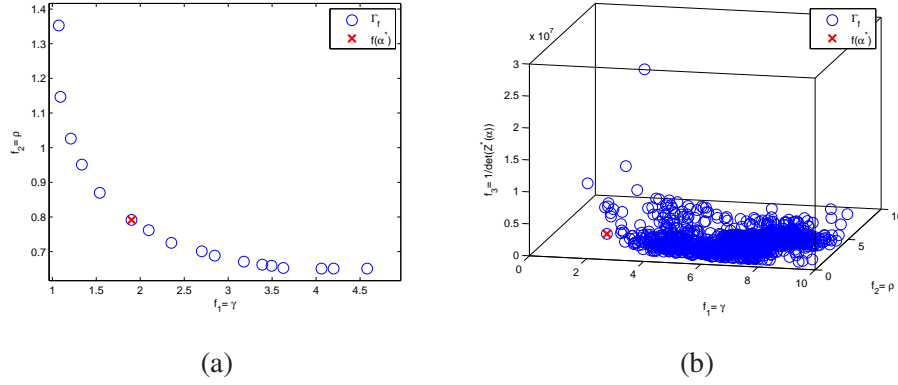


Fig. 3. APFs in Example 1: (a) the APF resulting from solving (14) and (b) the APF resulting from solving (15). Both cases show that the proposed HMODE algorithm can yield a reasonable tradeoff design represented by a knee $f(\alpha^*)$ of the APF Γ_f .

which are known to the designer. The nonlinear system (31) has been interpolated by a fuzzy system in (6) with $\mathcal{N}_r = 2$ and [35]

$$\begin{aligned} \xi_1(x_1(t)) &= \max\{\min\{-\frac{1}{50} \times (x_1(t) - 30), 1\}, 0\}, \xi_2(x_1(t)) = \max\{\min\{\frac{1}{50} \times (x_1(t) + 20), 1\}, 0\} \\ \mathbf{A}_1 &= \begin{bmatrix} -10 & 10 & 0 \\ 28 & -1 & 20 \\ 0 & -20 & -8/3 \end{bmatrix}, \mathbf{A}_2 = \begin{bmatrix} -10 & 10 & 0 \\ 28 & -1 & -30 \\ 0 & 30 & -8/3 \end{bmatrix}, \mathbf{B}_{1_1} = \mathbf{B}_{1_2} = \begin{bmatrix} 0.1 & 0 & 0 \\ 0 & 0.1 & 0 \\ 0 & 0 & 0.1 \end{bmatrix}, \mathbf{B}_{2_1} = \mathbf{B}_{2_2} = \begin{bmatrix} 1 \\ 0 \\ 0 \end{bmatrix}, \\ \mathbf{C}_1 = \mathbf{C}_2 &= \begin{bmatrix} 1 & 0 & 0 \\ 0 & 1 & 0 \\ 0 & 0 & 1 \end{bmatrix}, \mathbf{D}_1 = \mathbf{D}_2 = \begin{bmatrix} 1 \\ 1 \\ 1 \end{bmatrix}, \text{ and } \mathbf{H}_1 = \mathbf{H}_2 = \begin{bmatrix} -3 & 3 & 0 \\ 8.4 & 0 & 0 \\ 0 & 0 & -0.8 \end{bmatrix}. \end{aligned} \quad (33)$$

The range of interest

$$\boldsymbol{\alpha} \in [0.5, 5] \times [0.5, 5] \times [0.01, 5]$$

has been chosen, i.e.,

$$\underline{\boldsymbol{\alpha}} = [0.5 \quad 0.5 \quad 0.01]^T \text{ and } \bar{\boldsymbol{\alpha}} = [5 \quad 5 \quad 5]^T.$$

Solving (14) produced the APF in Fig. 3(a). The solution

$$\boldsymbol{\alpha}^* = [1.9009 \quad 0.7914 \quad 0.1585]^T$$

has been selected, which corresponds to the gain matrices

$$\mathbf{K}_1^*(\boldsymbol{\alpha}^*) \approx \mathbf{K}_2^*(\boldsymbol{\alpha}^*) \approx \begin{bmatrix} -1785 & -526.5 & 18.3 \end{bmatrix}. \quad (34)$$

Several points should be addressed here. First, while the values $\delta = 1$ and $\rho = 1$ were heuristically prescribed in [35], they were evaluated through an optimisation process in our MO approach, which should be better in general. Second, the shape of the APF in Fig. 3(a) shows how the tolerance of uncertainty

and the attenuation level affect each other: the objectives are dependent and conflicting, and the designer must trade off any improvement of one objective with the deterioration of the other objective. As shown in Fig. 3(a), the proposed approach can provide a reasonable design that corresponds to the nondominated vector $\mathbf{f}(\boldsymbol{\alpha}^*)$ lying in the knee region of the APF. This illustrates the validity of using (28). Finally, the resulting gain matrices in (34) can be too large, which is often undesired in practical applications.

To avoid obtaining large $\mathbf{K}_i^*(\boldsymbol{\alpha})$, the MOMIP (15) has been solved, yielding the new solution

$$\boldsymbol{\alpha}^* = \begin{bmatrix} 2.0900 & 2.6961 & 0.1469 \end{bmatrix}^T$$

and the gain matrices

$$\mathbf{K}_1^*(\boldsymbol{\alpha}^*) = \begin{bmatrix} -105.4586 & -34.9714 & 1.7917 \end{bmatrix}, \text{ and } \mathbf{K}_2^*(\boldsymbol{\alpha}^*) = \begin{bmatrix} -105.4506 & -34.9705 & 1.8222 \end{bmatrix}. \quad (35)$$

The values of $\mathbf{K}_1^*(\boldsymbol{\alpha}^*)$ and $\mathbf{K}_2^*(\boldsymbol{\alpha}^*)$ in (35) have been reduced compared with those in (34). Fig. 3(b) shows the corresponding APF.

For the chaotic system (31), we have chosen

$$\mathbf{x}(0) = \begin{bmatrix} x_1(0) & x_2(0) & x_3(0) \end{bmatrix}^T = \begin{bmatrix} 0 & 0 & 0 \end{bmatrix}^T, \sigma = \sigma(t) = 10 + \sin(t), r = 0.8 \times 28, b = 1.1 \times 8/3$$

$$w_1(t) = \text{rand}_{(-0.2,0.8)}(t), w_2(t) = \text{rand}_{(-0.7,1)}(t), w_3(t) = \text{rand}_{(-0.1,0.3)}(t)$$

and used the control law

$$u(t) = \xi_1(x_1(t))\mathbf{K}_1^*(\boldsymbol{\alpha}^*)\mathbf{x}(t) + \xi_2(x_1(t))\mathbf{K}_2^*(\boldsymbol{\alpha}^*)\mathbf{x}(t) \quad (36)$$

in our simulations. Figs. 4(a), (b), and (c) show the uncontrolled states, the controlled states using $\mathbf{K}_i^*(\boldsymbol{\alpha}^*)$ in (34), and the controlled states using $\mathbf{K}_i^*(\boldsymbol{\alpha}^*)$ in (35), respectively. It is clear that the uncontrolled states are bounded away from zero. In contrast, we have the controlled states $x_1(t) \approx x_2(t) \approx x_3(t) \approx 0$. The system states in this example have been effectively controlled, illustrating the validity of the proposed MO design. Furthermore, referring to Figs. 4(b) and (c) associated with the controller gains in (34) and (35), respectively, we conclude that our MO approach can reduce “the values of gain matrices” by adding an additional term to the objective function as in (15) while maintaining excellent performance of the controlled system.

B. Example 2: BIBO System Design

For the linear system in (16), the following values have been chosen in our simulations:

$$\mathbf{x}(0) = \begin{bmatrix} 3 \\ -4 \end{bmatrix}, \mathbf{A} = \begin{bmatrix} -10 & -5 \\ -4 & -1.2 \end{bmatrix}, \mathbf{B} = \begin{bmatrix} 3 & 1 \\ 0 & 2 \end{bmatrix}, \text{ and } \mathbf{C} = \begin{bmatrix} 1 & 0.7 \end{bmatrix}.$$

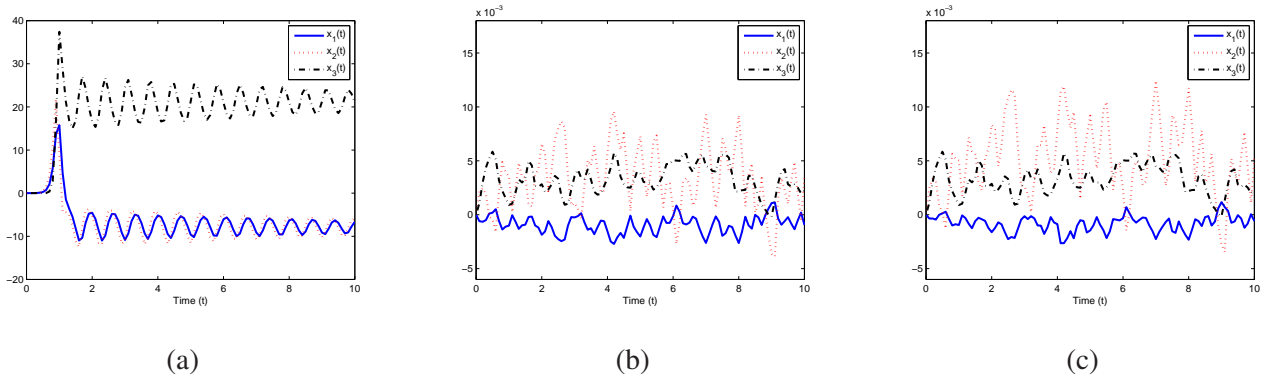


Fig. 4. Comparison between uncontrolled and controlled states in Example 1: (a) $u(t) = 0$; (b) $u(t)$ constructed according to (36) with $\mathbf{K}_i^*(\alpha)$ in (34); and (c) $u(t)$ constructed according to (36) with $\mathbf{K}_i^*(\alpha)$ in (35). Note that the scale along the y-axis in (b) and (c) is 10^{-3} . While the uncontrolled states in (a) are bounded away from the zero, the controlled states in (b) and (c) vibrate around the zero with very small amplitudes, indicating that the proposed MO design approach can yield feasible control laws. Although the differences between (b) and (c) are insignificant, the associated controller gains in (c) are smaller than those in (b).

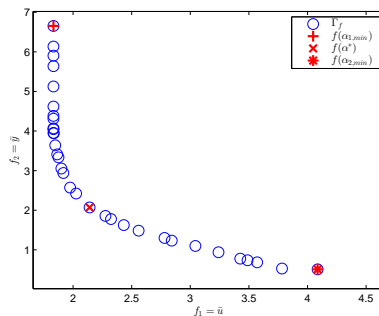


Fig. 5. APF Γ_f in Example 2. Three designs, denoted by $\alpha_{1,min}$, α^* and $\alpha_{2,min}$, have been selected for comparison. The designs $\alpha_{1,min}$ and $\alpha_{2,min}$ aim to minimise the upper bounds on the input norm $\|\mathbf{u}(t)\|$ and the output norm $\|\mathbf{y}(t)\|$, respectively. In contrast, the proposed MO approach yields the design α^* lying in the knee region of the APF, which corresponds to a tradeoff solution that sacrifices both objectives to some degree in order to do well on the whole.

Fig. 5 presents the APF resulting from solving (18). The APF shows that better performance (small \bar{y}) comes from the cost of using more input energy (large \bar{u}). The nondominated vector

$$\mathbf{f}(\alpha^*) = \alpha^* = \begin{bmatrix} 2.1412 & 2.0705 \end{bmatrix}^T$$

TABLE I
PERFORMANCE COMPARISON OF THE THREE TRADEOFF DESIGNS

Performance Index \ Design	$\alpha_{1,min}$	α^*	$\alpha_{2,min}$
$\max_t \ \mathbf{u}(t)\ $	1.7674	1.8906	3.6689
$\max_t y(t) $	1.0476	0.8751	0.2000

has been selected, leading to the controller gain

$$\mathbf{K}^*(\alpha^*) = \begin{bmatrix} -0.2037 & 0.0363 \\ 0.0168 & -0.4106 \end{bmatrix}.$$

We compared the selected design to two “extreme” designs denoted by

$$\alpha_{1,min} = \begin{bmatrix} 1.8324 & 6.6537 \end{bmatrix}^T \text{ and } \alpha_{2,min} = \begin{bmatrix} 4.0862 & 0.5084 \end{bmatrix}^T$$

as shown in Fig. 5. The corresponding gain matrices are

$$\mathbf{K}^*(\alpha_{1,min}) = \begin{bmatrix} -0.0813 & 0.1873 \\ 0.0979 & -0.2918 \end{bmatrix} \text{ and } \mathbf{K}^*(\alpha_{2,min}) = \begin{bmatrix} -3.0274 & -2.3897 \\ 0.0858 & -0.7900 \end{bmatrix}.$$

Table I summarizes the performance of the three designs, i.e., α^* , $\alpha_{1,min}$, and $\alpha_{2,min}$. As expected, the design $\alpha_{1,min}$ leads to the smallest $\max_t \|\mathbf{u}(t)\|$ because it aims at minimising the upper bound \bar{u} on $\|\mathbf{u}(t)\|$. The design $\alpha_{2,min}$ leads to the smallest $\max_t |y(t)|$ as this design focuses on the minimisation of the upper bound \bar{y} on $|y(t)|$. In contrast, the proposed approach provides a trade-off design that sacrifices both objectives to some degree in order to do well on the whole.

VI. CONCLUSION

In this paper, linear matrix inequality (LMI) approaches have been extended to address controller design problems with multiple objectives. A hybrid multiobjective differential evolution (HMODE) algorithm, a type of multiobjective evolutionary algorithms (MOEAs), has been proposed. Although LMI approaches and the development of MOEAs are mature, we have integrated them for multiobjective (MO) controller designs, which has not been thoroughly investigated in the literature. Several benefits of using the integration are summarized as follows. First, Pareto optimality for MO controller designs can be achieved in a systematic way. This is done by solving an MO matrix inequality problem (MOMIP) using the HMODE algorithm. Second, a system designer can have a clear view on how objectives affect each other. This comes from the availability of an approximated Pareto front (APF) produced by solving the

MOMIP. In this case, a broad perspective on the optimality can be obtained as compared to conventional SO designs. Third, if the shape of the APF is bent, then it is possible to select the “optimal” trade-off controller: all objectives are sacrificed to some degree but the system performance is improved on the whole, i.e., a win-win situation can be created. Fourth, design parameters can be selected through optimisation without using a heuristic assignment. Finally, our MO design approach can adjust the values of controller gains by adding an additional term to the cost function, showing its flexibility.

REFERENCES

- [1] She, Y., Baran, M.E., She, X.: ‘Multiobjective control of PEM fuel cell system with improved durability’, *IEEE Trans. Sustainable Energy*, 2013, 4, (1), pp. 127–135
- [2] Chipperfield, A.J., Bica, B., Fleming, P.J.: ‘Fuzzy scheduling control of a gas turbine aero-engine: A multiobjective approach’, *IEEE Trans. Ind. Electron.*, 2002, 49, (3), pp. 536–548
- [3] Wojsznis, W., Mehta, A., Wojsznis, P., Thiele, D., Blevins, T.: ‘Multi-objective optimization for model predictive control’, *ISA Transactions*, 2007, 46, (3), pp. 351–361
- [4] Wang, Z., Zeng, H., Ho, D.W.C., Unbehauen, H.: ‘Multiobjective control of a four-link flexible manipulator: A robust H_∞ approach’, *IEEE Trans. Control Syst. Technol.*, 2002, 10, (6), pp. 866–875
- [5] Yang, C., Zhang, Q.: ‘Multiobjective control for T-S fuzzy singularly perturbed systems’, *IEEE Trans. Fuzzy Syst.*, 2009, 17, (1), pp. 104–115
- [6] Lin, C.-L., Jan, H.-Y., Shieh, N.-C.: ‘GA-based multiobjective PID control for a linear brushless DC motor’, *IEEE/ASME Trans. Mechatronics*, 2003, 8, (1), pp. 56–65
- [7] Ebihara, Y., Hagiwara, T.: ‘New dilated LMI characterizations for continuous-time control design and robust multiobjective control’. *Proc. American Control Conference*, Anchorage, AK, May 2002, pp. 47–52
- [8] Chen, H., Guo, K.: ‘An LMI approach to multiobjective RMS gain control for active suspensions’. *Proc. American Control Conference*, Arlington, VA, Jun. 2001, pp. 2646–2651
- [9] Shimomura, T., Fujii, T.: ‘Multiobjective control design via successive over-bounding of quadratic terms’. in *Proc. IEEE Conference on Decision and Control*, Sydney, Australia, Dec. 2000, pp. 2763–2768
- [10] Tanaka, K., Hori, S., Wang, H.O.: ‘Multiobjective control of a vehicle with triple trailers’, *IEEE/ASME Trans. Mechatronics*, 2002, 7, (3), pp. 357–368
- [11] Tseng, C.-S., Chen, B.-S.: ‘Multiobjective PID control design in uncertain robotic systems using neural network elimination scheme’, *IEEE Trans. Syst., Man, Cybern. A*, 2001, 31, (6), pp. 632–644
- [12] Heo, J.S., Lee, K.Y., Garduno-Ramirez, R.: ‘Multiobjective control of power plants using particle swarm optimization techniques’, *IEEE Trans. Energy Convers.*, 2006, 21, (2), pp. 552–561
- [13] Lu, J., DePoyster, M.: ‘Multiobjective optimal suspension control to achieve integrated ride and handling performance’, *IEEE Trans. Control Syst. Technol.*, 2002, 10, (6), pp. 807–821
- [14] Elmusrati, M., Janti, R., Koivo, H.N.: ‘Multiobjective distributed power control algorithm for CDMA wireless communication systems’, *IEEE Trans. Veh. Technol.*, 2007, 56, (2), pp. 779–788
- [15] Yang, C.-Y., Chen, B.-S., Jian, C.-Y.: ‘Robust two-loop power control for CDMA systems via multiobjective optimization’, *IEEE Trans. Veh. Technol.*, 2012, 61, (5), pp. 2145–2157

- [16] Audet, C., Savard, G. Zghal, W.: ‘Multiobjective optimization through a series of single-objective formulations’, *SIAM J. Optim.*, 2008, 19, (1), pp. 188–210
- [17] Coello, C.A.C., Van Veldhuizen, D.A., Lamont, G.B.: ‘Evolutionary Algorithms for Solving Multi-objective Problems’ (Kluwer Academic, New York, 2002)
- [18] Lin, C.-T., Chung, I.-F.: ‘A reinforcement neuro-fuzzy combiner for multiobjective control’, *IEEE Trans. Syst., Man, Cybern. B*, 1999, 29, (6), pp. 726–744
- [19] Abbaszadeh, M., Marquez, H.J.: ‘LMI optimization approach to robust H_∞ observer design and static output feedback stabilization for discrete-time nonlinear uncertain systems’, *International Journal of Robust and Nonlinear Control*, 2009, 19, (3), pp. 313–340
- [20] Abbaszadeh, M., Marquez, H.J.: ‘Nonlinear robust H-infinity filtering for a class of uncertain systems via convex optimization’, *Journal of Control Theory and Applications*, 2012, 10, (2), pp. 152–158
- [21] Patnaik, A., Behera, L.: ‘Evolutionary multiobjective optimization based control strategies for an inverted pendulum on a cart’. *Proc. IEEE Congress on Evolutionary Computation*, Hong Kong, China, Jun. 2008, pp. 3141–3147
- [22] Ma, H.M., Ng, K.-T., Man, K.F.: ‘Multiobjective coordinated power voltage control using jumping genes paradigm’, *IEEE Trans. Ind. Electron.*, 2008, 55, (11), pp. 4075–4084
- [23] Aggelogiannaki, E., Sarimveis, H.: ‘A simulated annealing algorithm for prioritized multiobjective optimization-implementation in an adaptive model predictive control configuration’, *IEEE Trans. Syst., Man, Cybern. B*, 2007, 37, (4), pp. 902–915
- [24] Fazzolari, M., Alcalá, Nojima, R.Y., Ishibuchi, H., Herrera, F.: ‘A review of the application of multiobjective evolutionary fuzzy systems: Current status and further directions’, *IEEE Trans. Fuzzy Syst.*, 2013, 21, (1), pp. 45–65
- [25] Boyd, S., El Ghaoui, L., Feron, E., Balakrishnan, V.: ‘*Linear Matrix Inequalities in System and Control Theory*’ (SIAM, Philadelphia, 1994)
- [26] Wan, Z., Kothare, M.V.: ‘An efficient off-line formulation of robust model predictive control using linear matrix inequalities’, *Automatica*, 2003, 39, (5), pp. 837–846
- [27] Kothare, M.V., Balakrishnan, V., Morari, M.: ‘Robust constrained model predictive control using linear matrix inequalities’, *Automatica*, 1996, 32, (10), pp. 1361–1379
- [28] Chiu, W.-Y., Chen, B.-S.: ‘Multisource prediction under nonlinear dynamics in WSNs using a robust fuzzy approach’, *IEEE Trans. Circuits Syst. I*, 2011, 58, (1), pp. 137–149
- [29] Chiu, W.-Y., Chen, B.-S., Poor, H.V.: ‘A multiobjective approach for source estimation in fuzzy networked systems’, *IEEE Trans. Circuits Syst. I*, 2013, 60, (7), pp. 1890–1900
- [30] Tanaka, K., Wang, H.O.: ‘*Fuzzy Control Systems Design and Analysis: A Linear Matrix Inequality Approach*’ (Wiley-Interscience, New York, 2001)
- [31] Ho, W.-H., Tsai, J.-T., Chou, J.-H.: ‘Robust quadratic-optimal control of TS-fuzzy-model-based dynamic systems with both elemental parametric uncertainties and norm-bounded approximation error’, *IEEE Trans. Fuzzy Syst.*, 2009, 17, (3), pp. 518–531
- [32] Lin, C.-M., Li, H.-Y.: ‘TSK fuzzy CMAC-based robust adaptive backstepping control for uncertain nonlinear systems’, *IEEE Trans. Fuzzy Syst.*, 2012, 20, (6), pp. 1147–1154
- [33] Ho, W.-H., Chou, J.-H.: ‘Robust finite-time optimal linear state feedback control of uncertain TS-fuzzy-model-based control systems’. *Proc. IEEE International Conference on Systems, Man and Cybernetics*, Taipei, Taiwan, Oct. 2006, pp. 2590–2595

- [34] Lee, H.J., Park, J.B., Chen, G.: ‘Robust fuzzy control of nonlinear systems with parametric uncertainties’, *IEEE Trans. Fuzzy Syst.*, 2001, 9, (2), pp. 369–379
- [35] Assawinchaichote, W., Nguang, S.K., Shi, P.: ‘Fuzzy Control and Filter Design for Uncertain Fuzzy Systems’ (Springer-Verlag GmbH, Berlin Heidelberg, 2006)
- [36] Henrion, D., Korda, M.: ‘Convex computation of the region of attraction of polynomial control systems’, *IEEE Trans. Autom. Control*, 2014, 59, (2), pp. 297–312
- [37] Lee, D., Joo, H.Y.H., Tak, M.H.: ‘Linear matrix inequality approach to local stability analysis of discrete-time Takagi-Sugeno fuzzy systems’, *IET Control Theory and Applications*, 2013, 7, (9), pp. 1309–1318
- [38] Bender, F.A., Gomes da Silva, J.M., Tarbouriech, S.: ‘Convex framework for the design of dynamic anti-windup for state-delayed systems’, *IET Control Theory and Applications*, 2011, 5, (12), pp. 1388–1396
- [39] Forbes, J.R.: ‘Dual approaches to strictly positive real controller synthesis with a H_2 performance using linear matrix inequalities’, *Int. J. Robust. Nonlinear Control*, 2013, 23, (8), pp. 903–918
- [40] Sadeghzadeh, A.: ‘Identification and robust control for systems with ellipsoidal parametric uncertainty by convex optimization’, *Asian Journal of Control*, 2012, 14, (5), pp. 1251–1261
- [41] Poursafar, N., Taghirad, H.D., Haeri, M.: ‘Model predictive control of non-linear discrete time systems: a linear matrix inequality approach’, *IET Control Theory and Applications*, 2010, 4, (10), pp. 1922–1932
- [42] Santana-Quintero, L.V., Coello, C.A.C.: ‘An algorithm based on differential evolution for multi-objective problems’, *International Journal of Computational Intelligence Research*, 2005, 1, (2), pp. 151–169
- [43] Hernandez-Diaz, A.G., Santana-Quintero, L.V., Coello, C.C., Caballero, R., Molina, J.: ‘A new proposal for multi-objective optimization using differential evolution and rough sets theory’. *Proc. Genetic and Evolutionary Computation Conference*, Seattle, WA, Jul. 2006, pp. 675–682
- [44] Zhang, J., Sanderson, A.C.: ‘JADE: Adaptive differential evolution with optional external archive’, *IEEE Trans. Evol. Comput.*, 2009, 13, (5), pp. 945–958
- [45] Hsieh, M.-N., Chiang, T.-C., Fu, L.-C.C.: ‘A hybrid constraint handling mechanism with differential evolution for constrained multiobjective optimization’. *Proc. IEEE Congress on Evolutionary Computation*, New Orleans, LA, Jun. 2011, pp. 1785–1792
- [46] Wang, Y. and Cai, Z.: ‘Combining multiobjective optimization with differential evolution to solve constrained optimization problems’, *IEEE Trans. Evol. Comput.*, 2012, 16, (1), pp. 117–134